Supporting Information

Delta-temperatural electronic transportations achieved in metastable perovskites rare-earth nickelates thin films

Jikun Chen[1], Haiyang Hu[1], Takeaki Yajima[2], Jiaou Wang[3], Binghui Ge[4], Hongliang Dong[5], Yong Jiang[1], and Nuofu Chen[6]

[1]Beijing Advanced Innovation Center for Materials Genome Engineering, School of Materials Science and Engineering, University of Science and Technology Beijing, Beijing 100083, China

[2]School of Engineering, The University of Tokyo, 2-11-16 Yayoi, Bunkyo-ku, Tokyo 113-0032, Japan

[3]Beijing Synchrotron Radiation Facility, Institute of High Energy Physics, Chinese Academy of Sciences, Beijing 100049, China

[4]Institute of Physical Science and Information Technology, Anhui University, 230601, Heifei, Anhui, China

[5]Center for High Pressure Science and Technology Advanced Research, Shanghai 201203, China

[6]School of Renewable Energy, North China Electric Power University, Beijing 102206, China

Correspondence: Prof. Jikun Chen (jikunchen@ustb.edu.cn), Prof. Yong Jiang (yjiang@ustb.edu.cn) and Prof. Nuofu Chen (nfchen@ncepu.edu.cn); Request for materials: Prof. Jikun Chen (jikunchen@ustb.edu.cn).

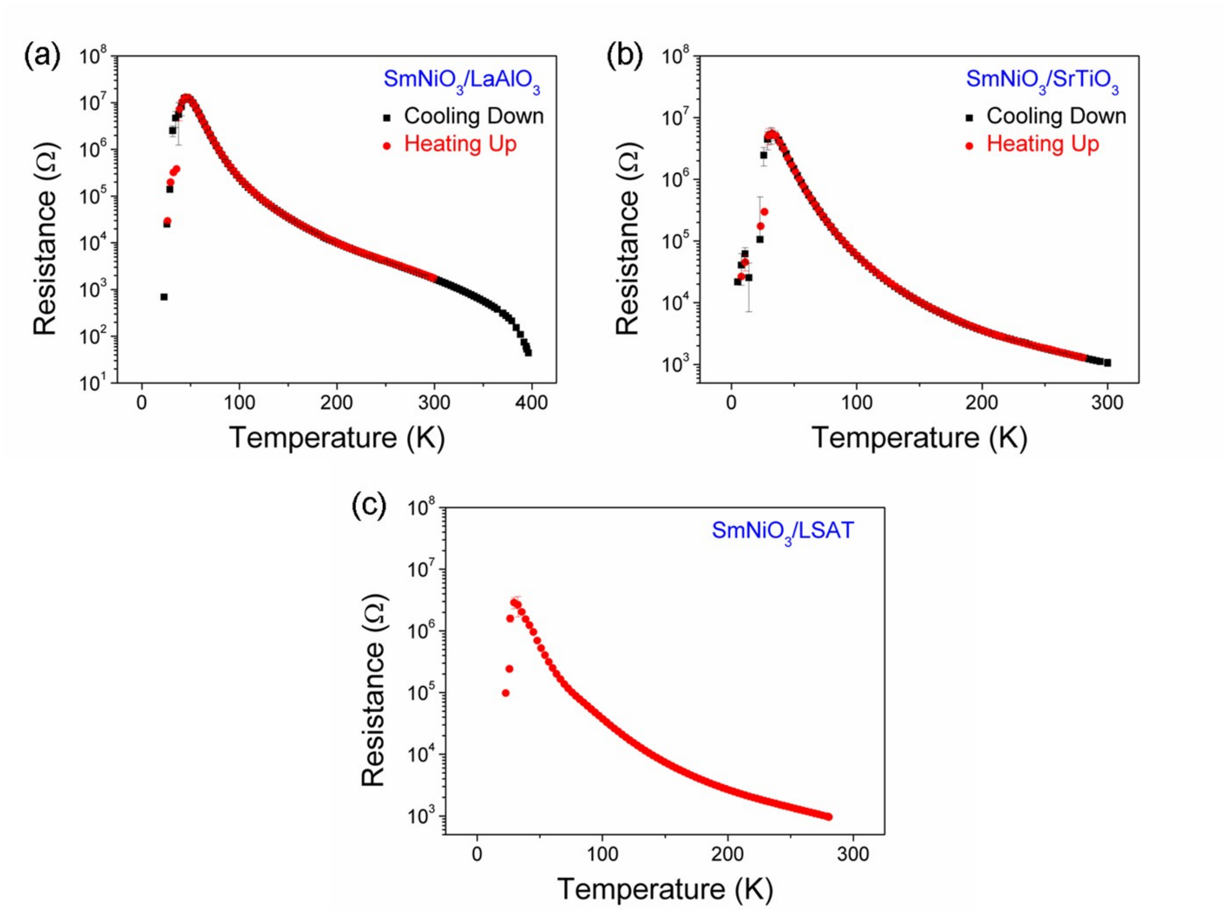

Figure S1. The resistance of $SmNiO_3$ (SNO) on **(a)** $LaAlO_3$ (LAO), **(b)** $SrTiO_3$ (STO) and **(c)** $(LaAlO_3)_{0.3}(Sr_2AlTaO_6)_{0.7}$ (LSAT) substrates with a (001) orientation measured as a function of temperature.

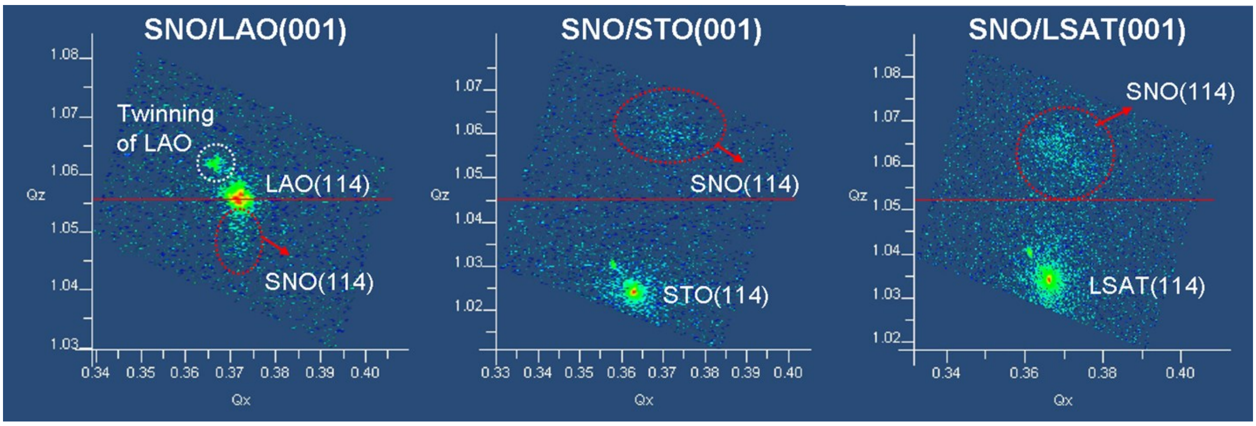

Figure S2. The X-ray reciprocal space mapping of $SmNiO_3$ (SNO) grown on single crystalline perovskite structured substrates, such as $LaAlO_3$ (LAO), $SrTiO_3$ (STO) and $(LaAlO_3)_{0.3}(Sr_2AlTaO_6)_{0.7}$ (LSAT) with (001) orientation via the chemical approach reported previously. The reciprocal vector of (114) is used to probe the diffraction patterns from both the thin film and the substrate.

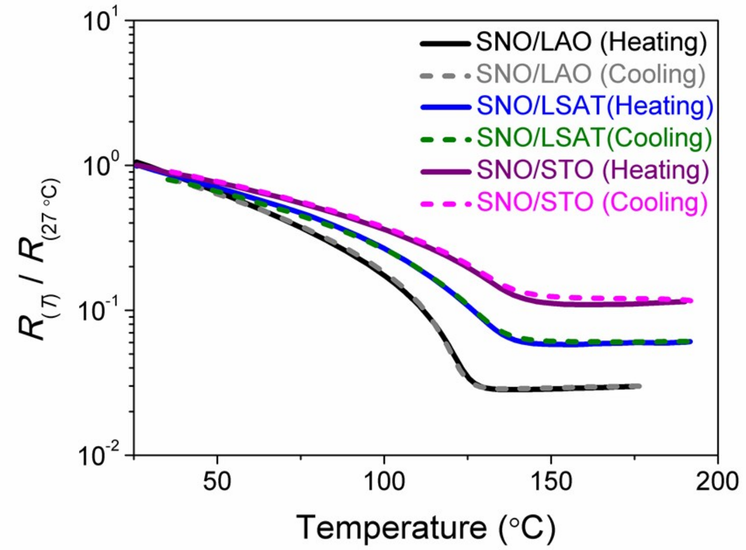

Figure S3. The temperature dependence in resistivity for $SmNiO_3/LaAlO_3$, $SmNiO_3/SrTiO_3$, and $SmNiO_3/(La,Sr)(Al,Ta)O_3$, measured via heating up (solid lines) and cooling down (dash lines). A lower metal to insulator transition temperature (T_{MIT}) is observed for the bi-axial distorted $SmNiO_3/(La,Sr)(Al,Ta)O_3$, compared to the partially tensile strain relaxed $SmNiO_3/SrTiO_3$, and $SmNiO_3/(La,Sr)(Al,Ta)O_3$. These observations are in agreement to the previous reports on strain distorted $SmNiO_3$.

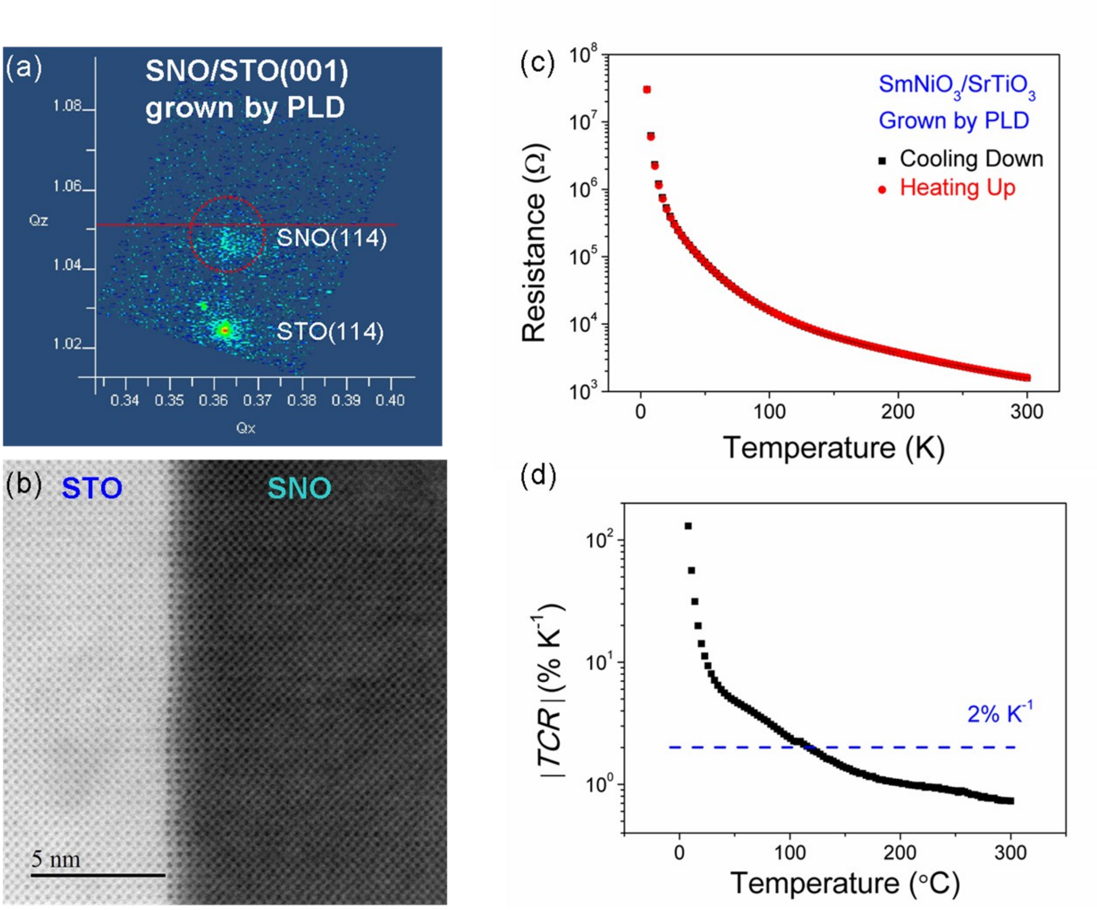

Figure S4. (a) The X-ray reciprocal space mapping of $SmNiO_3$ (SNO) grown on single crystalline $SrTiO_3$ (STO) with (001) orientation via pulsed laser deposition. The reciprocal vector of (114) is used to probe the diffraction patterns from both the thin film and the substrate. **(b)** The interfacial morphology of as-grown $SmNiO_3$ /$SrTiO_3$ from the high-angle annular dark-field (HAADF) images. **(c)** Temperature dependence of the resistivity and **(d)** Temperature coefficients of resistance (TCR) for as-grown $SmNiO_3$/$SrTiO_3$.

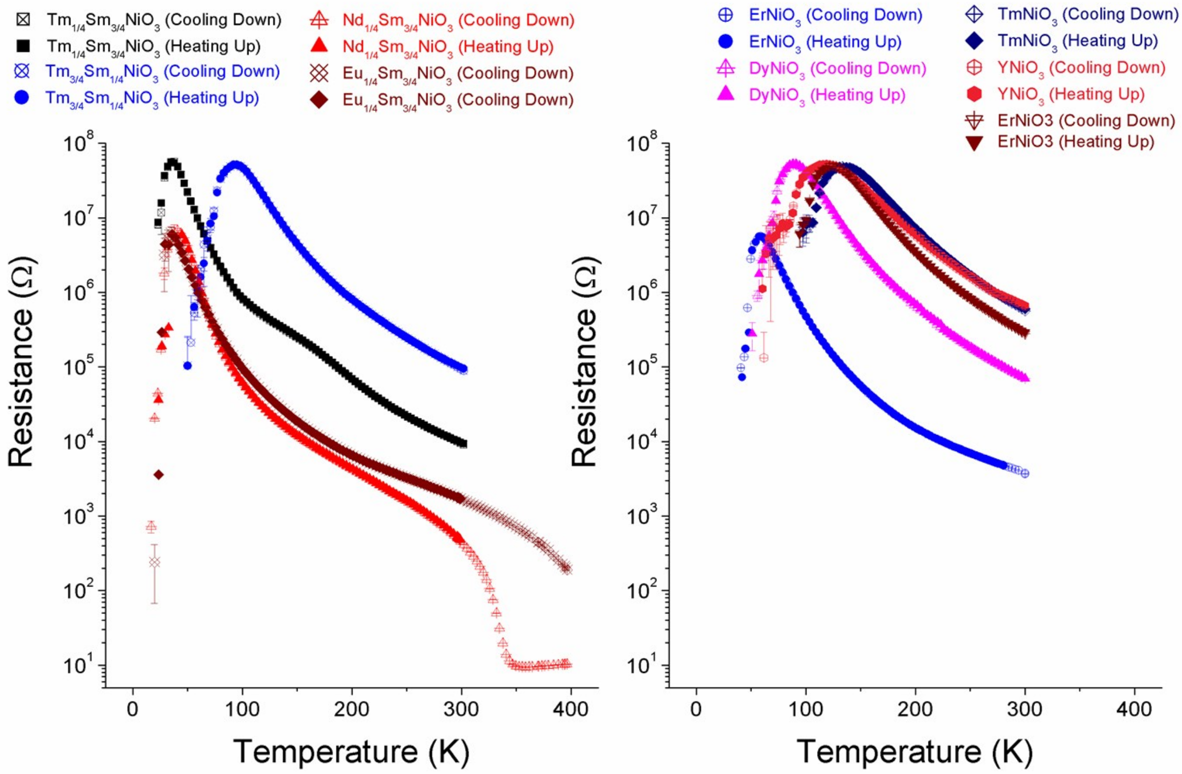

Figure S5. The resistance of *Re*NiO_3 grown on the $LaAlO_3$ (001) substrate with single and multiple rare earth compositions measured as a function of temperature.

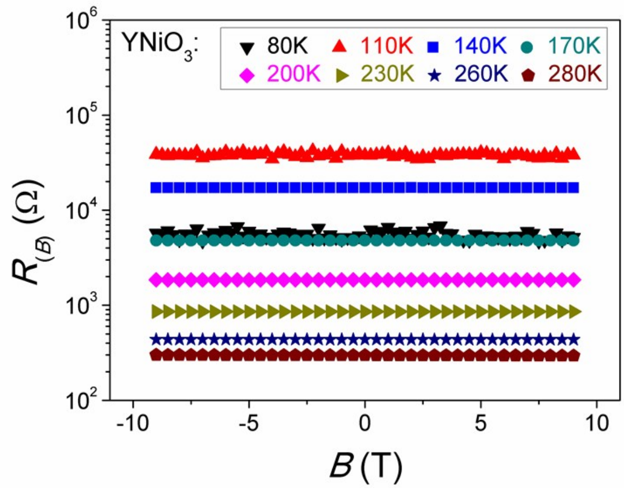

Figure S6. Resistance of $YNiO_3$ measured as a function of the imparted external magnetic fields (B) at various temperatures.

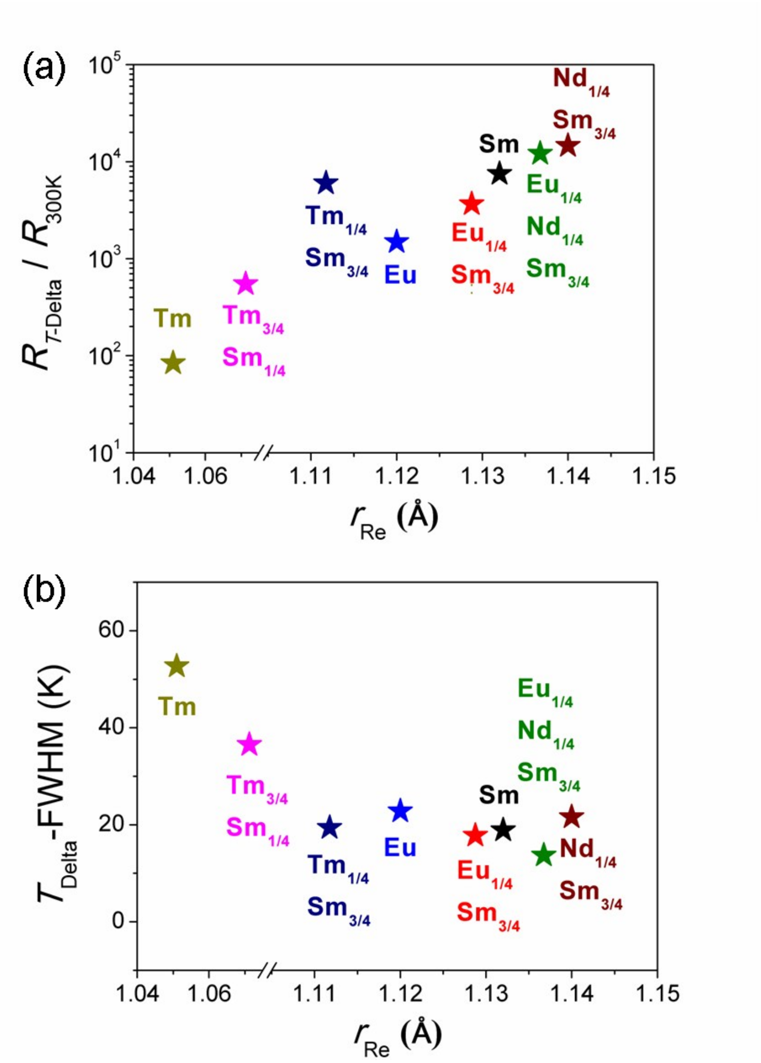

Figure S7. (a) The maximum resistivity at $T_{\text{R-MIT}}$ compared to the one at 300 K, and **(b)** the full widths half maximum of its resultant delta-shaped temperature dependence in resistivity (T_{Delta}-FWHM) summarized from the *R*-*T* of multiple rare-earth composition perovskite nickelates shown in Figure 4a.